

ORIGINAL RESEARCH ARTICLE

Marked dysregulation of mature 3p and 5p arms of miR-182 and miR-490 lacks prognostic value for 5-year survival in colorectal cancer

Arash Moradi¹ , Seyedeh Hanieh Safavi Komamardakhi¹ ,
Ramtin Mohammadi¹ , Majid Pornour² , Azar Heidarizadi¹ ,
Mahmoud Hatami¹ , Mariasanta Napolitano^{3*} , and
Shahla Mohammad Ganji^{1*} 

¹Department of Molecular Medicine, Medical Biotechnology Institute, National Institute of Genetic Engineering and Biotechnology, Tehran, Iran

²Jeanie and Tony Loop Laboratory for Immuno-Oncology, Lombardi Comprehensive Cancer Center, Georgetown University Medical Center, Pre-Clinical Science Building, Washington DC, United States of America

³Department of Health Promotion, Maternal-Childhood, Internal Medicine of Excellence G.D'Alessandro, University of Palermo, Palermo, Italy

*Corresponding authors:

Shahla Mohammad Ganji
(shahla@nigeb.ac.ir);
Mariasanta Napolitano
(marysanta@libero.it)

Citation: Moradi A, Komamardakhi SHS, Mohammadi R. Marked dysregulation of mature 3p and 5p arms of miR-182 and miR-490 lacks prognostic value for 5-year survival in colorectal cancer. *Eurasian J Med Oncol.* 2026;10(1):306-317. doi: 10.36922/EJMO025410432

Received: October 10, 2025

Revised: December 5, 2025

Accepted: January 6, 2026

Published online: February 3, 2026

Copyright: © 2026 Author(s). This is an Open-Access article distributed under the terms of the Creative Commons Attribution License, permitting distribution, and reproduction in any medium, provided the original work is properly cited.

Publisher's Note: AccScience Publishing remains neutral with regard to jurisdictional claims in published maps and institutional affiliations.

Abstract

Introduction: Colorectal cancer (CRC) is a leading cause of cancer mortality. MicroRNAs are key regulators of gene expression implicated in carcinogenesis. While miR-182 is an established oncomiR and miR-490 acts as a tumor suppressor, the prognostic significance of their mature arms (–3p/–5p) remains unclear.

Objective: This study aims to validate these mature arms in CRC and assess their association with 5-year overall survival.

Methods: We combined bioinformatics with experimental validation in 48 CRC patients. Putative targets were analyzed for their involvement in biological pathways. Expression levels were quantified in tumor and paired normal tissues using quantitative PCR. Associations with survival were evaluated using Kaplan–Meier and Cox proportional hazards models.

Results: Bioinformatics linked miR-182 targets to cell movement and miR-490 to the mitotic cell cycle. In patient tissues, miR-182-5p (fold change [FC]: 16.19) and miR-182-3p (FC: 3.38) were significantly upregulated ($p < 0.05$). Conversely, miR-490-5p (FC: 0.26) and miR-490-3p (FC: 0.76) were significantly downregulated ($p < 0.05$). Despite this dysregulation, multivariate Cox models showed no significant association with 5-year survival. Hazard ratios (HR) lacked significance for both miR-182-5p (HR = 0.858, 95% CI: 0.610–1.205, $p = 0.377$) and miR-490-3p (HR = 0.665, 95% CI: 0.357–1.239, $p = 0.198$).

Conclusion: This study validates the opposing dysregulation of mature miR-182 and miR-490 arms in CRC, reinforcing their respective oncogenic and tumor-suppressive roles. However, these profound expression changes did not translate into prognostic utility for 5-year survival in this cohort, suggesting that larger high-throughput-based studies are required to detect putative prognostic effects.

Keywords: Colorectal neoplasms; Gene expression regulation; MicroRNAs; Neoplasm

1. Introduction

Colorectal cancer (CRC) represents a significant global health challenge, with approximately 1.9 million new cases diagnosed in 2022. While incidence rates are higher in developed countries, an alarming trend of rising CRC incidence is observed in transitioning nations, likely attributable to changes in lifestyle and diet. Furthermore, CRC cases are now rising among younger adults in high-income countries, underscoring the need to clarify the underlying causes of this trend.¹ Despite advancements in screening methods and the promotion of healthy lifestyle choices, researchers identify promising opportunities to reduce the global burden of CRC.² They emphasize the importance of increasing access to high-quality screening and treatment for all populations. Despite widespread efforts to improve CRC screening rates, at least 40% of age-eligible adults do not comply with screening procedures.² The new generation of non-invasive, molecular-based diagnostic tests with high sensitivity and specificity can enhance the assessment of cancer initiation, tumor progression, and treatment response.^{3,4}

CRC represents an etiologically heterogeneous disease based on tumor anatomical location and several different molecular alterations. Similar to other cancer types, the stepwise accumulation of genetic and epigenetic alterations in the normal colonic epithelial cells leads to colorectal adenomas and, ultimately, invasive adenocarcinomas.⁵ The consensus molecular subtypes (CMS) classification further delineates tumors into four categories based on immune activation, metabolic dysregulation, and mesenchymal traits, underscoring the need for precise biomarkers that can operate across or within these subtypes to predict patient outcomes.⁶ This refined classification system enhances our understanding of CRC's molecular diversity, paving the way for personalized medicine and targeted interventions.

Investigations have revealed that over 98% of the human genome comprises non-protein-coding sequences. This finding underscores the importance of non-coding regions and their potential impact.⁷ One important class of non-coding RNA (ncRNA) is microRNAs (miRNAs), which play critical roles in diverse developmental and cellular processes by regulating gene expression at the post-transcriptional level.^{8,9} Notably, miRNAs are commonly identified by differential expression profiling in cancerous tissues and compared to adjacent non-cancerous tissues.¹⁰⁻¹²

Mature miRNAs may be generated from the 5p or 3p arm of the pre-miRNA hairpin. Historically, one arm was considered the dominant “guide” strand while the other was degraded. However, increasing evidence indicates that both arms can generate functional, mature miRNAs with distinct

targetomes, depending on developmental stage or tissue type.¹³ Multiple mechanisms could cause dysregulation of miRNA expression,¹⁴ leading to perturbation of cellular homeostasis, thereby facilitating cancer development.¹⁵ As miRNAs play a crucial role in various biological processes, abnormal miRNA expression is likely to contribute to the regulation of cell cycle and death in tumorigenesis.¹⁶ For example, miR-218 induces G2-phase cell cycle arrest in colon cancer cells by inhibiting cyclin-dependent kinase 4 and increasing p53 levels.¹⁷ These observations provide compelling evidence for the influential role of miRNAs in modulating both cellular proliferation and apoptotic pathways (Figure 1). It is important to note that while high-throughput sequencing is necessary to distinguish specific mature arm sequence variants that differ by single nucleotides,¹⁸ stem-loop quantitative real-time polymerase chain reaction (RT-PCR) remains the gold standard for quantifying the abundance of the dominant mature miRNA species.¹⁹ The stem-loop primer confers specificity by targeting the mature 3' end of the miRNA, ensuring that the assay detects the canonical, functional arm.²⁰ Therefore, in this study, we independently quantified the dominant mature 3p and 5p products of the oncogenic miR-182 and tumor-suppressive miR-490 using stem-loop quantitative RT-PCR to dissect their specific contributions to CRC prognosis.

2. Materials and methods

2.1. Materials

The CRC cell lines SW480 (National Center for Biotechnology Information [NCBI] No. C506) and CACO-2 (NCBI No. C139) were obtained from the Pasteur Institute, Tehran, Iran. RiboEx™ reagent (Cat. No. 301-001, GeneAll Biotechnology Co., South Korea) was used to extract RNA from CRC tissues. Complementary DNA (cDNA) synthesis was performed using the AddScript cDNA Synthesis Kit (Cat. No. 23023, Addbio Meditech Co., South Korea). RT-PCR was performed using Ampliqon RT-PCR Master Mix (Ampliqon, Denmark) and RealQ plus 2X master mix green (Cat. No. A323402, Ampliqon, Denmark).

2.2. MicroRNA target prediction, signaling pathway analysis, and gene expression

Data on miRNA targets, including interactions with mRNAs, long ncRNAs, and proteins, were downloaded from the miRNet 2.0 repository (<https://www.mirnet.ca/>; accessed May 2023), using the *Homo sapiens* species setting.²¹ To identify high-confidence functional targets, we employed an intersection strategy that combines bioinformatics predictions with expression data. Putative targets were defined as genes that were both: (i) predicted

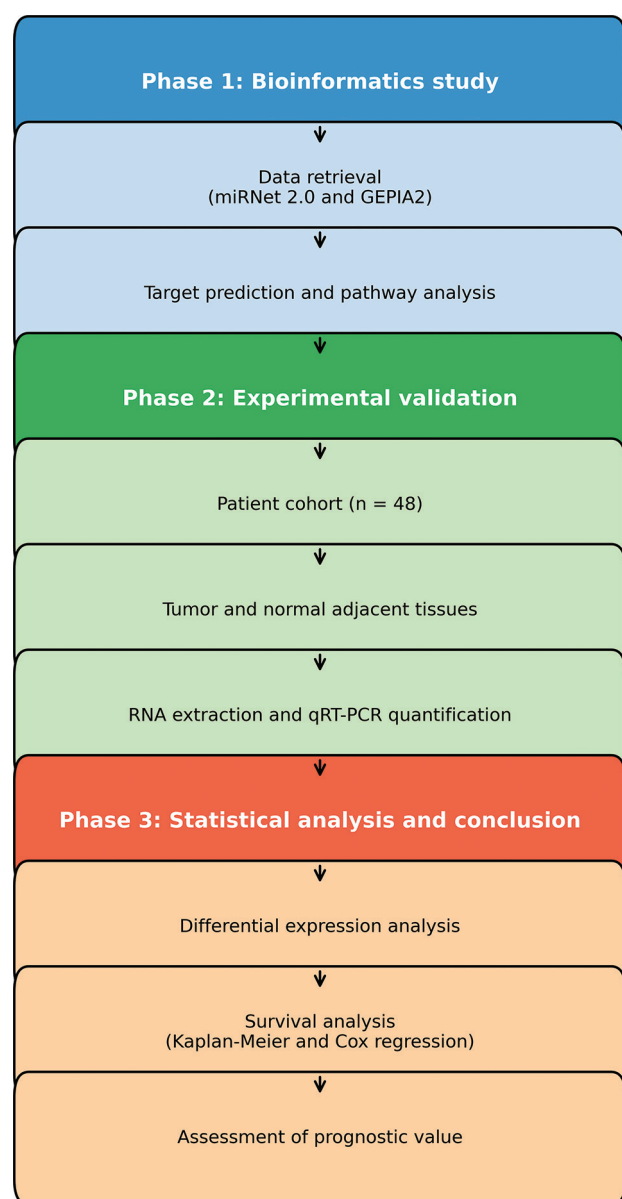


Figure 1. The study framework. This study comprises two components: bioinformatic analyses and experimental validation. Abbreviations: CRC: Colorectal cancer; GEPIA2: Gene Expression Profiling Interactive Analysis 2; GO: Gene ontology; KEGG: Kyoto Encyclopedia of Genes and Genomes; miRNA: MicroRNA; miRDB: MicroRNA database; NAT: Normal adjacent tissue; qRT-PCR: Quantitative real-time polymerase chain reaction.

by miRNet 2.0, and (ii) significantly differentially expressed in the Gene Expression Profiling Interactive Analysis 2 (GEPIA2) CRC dataset (<http://gepia2.cancer-pku.cn/>; accessed May 2023) with an inverse correlation to the miRNA.²² Specifically, for the upregulated mature miR-182, we intersected predicted targets with significantly downregulated genes in CRC; for the downregulated mature miR-490, we intersected targets with significantly

upregulated genes. The differential expression cutoffs in GEPIA2 were set at $|\log_2 \text{fold change (FC)}| > 1$ and $p < 0.01$. Functional enrichment analysis of the intersected target genes was performed using ShinyGO (0.77, South Dakota State University, USA; <http://bioinformatics.sdstate.edu/>). The signaling pathways potentially modulated by these targets were identified using the Kyoto Encyclopedia of Genes and Genomes pathways program.²³ Enrichment significance was calculated using a hypergeometric test against a background of all protein-coding genes, with false discovery rate (FDR) correction applied to account for multiple testing (FDR < 0.05).

2.3. Collection of cells and tissues

The study protocol was approved by the National Institute of Genetic Engineering and Biotechnology (NIGEB) Ethics Committee (Approval Number: NIGEB.EC.1397.8.1.G; dated 2018) and carried out in accordance with their guidelines. All patients provided written informed consent before participating. Ninety-six surgically resected colorectal specimens, including 48 CRC samples and 48 matched non-tumoral samples (histologically normal adjacent tissues [NATs] to the tumor), were included in this study. To minimize selection bias, the cohort consisted of consecutive patients diagnosed with primary CRC who underwent surgical resection. The specific inclusion criteria were: (i) Histologically confirmed colorectal adenocarcinoma; (ii) no history of pre-operative chemotherapy or radiotherapy (to avoid treatment-induced expression changes); (iii) availability of adequate paired tumor and NAT samples; and (iv) complete clinicopathological and follow-up data. Exclusion criteria included: (i) Diagnosis of hereditary CRC syndromes (e.g., FAP, HNPCC); and (ii) patients with a history of other synchronous or metachronous malignancies. Clinical follow-up data were retrieved from hospital medical records and cancer registry databases. Overall survival (OS) time was calculated as the interval from the date of surgical resection to the date of death or the date of last follow-up (Table 1). All fresh samples were frozen immediately after resection and stored at -70°C until use. Tumor samples were staged according to the most recent World Health Organization staging classification, published in 2019.²⁴

2.4. RNA extraction and relative quantitative RT-PCR analysis

Total RNA was extracted using RiboExTM reagent and assessed using 1% agarose gel electrophoresis and a spectrophotometer (NanoDropTM 2000, Thermo Scientific, USA). For cDNA synthesis, 1000 ng of total RNA was reverse-transcribed using the AddScript cDNA Synthesis Kit, which contains thermostable M-MLV Reverse

Transcriptase (RNase H-) and RNase inhibitors. Reverse transcription was performed as a single-cycle reaction: incubation at 50°C for 60 min, followed by inactivation of the enzyme at 80°C for 5 min. Quantitative RT-PCR was performed on a Mic qPCR Cycler (BMS-MIC-2, BMS, USA) using RealQ Plus 2X Master Mix Green (Ampliqon, Denmark) in 20 µL reactions containing 2 µL cDNA. The thermal cycling conditions were: initial activation at 95°C for 15 min, followed by 35 cycles of denaturation at 95°C for 15 s, annealing at 60°C for 15 s, and elongation at 72°C for 10 s (Table 2). Assay specificity and efficiency

Table 1. Demographic information of included patients

Demographic information	Category	No. (%)
Age (year)	Under 50	13 (28)
	Above 50	35 (72)
	Mean (range)	52 (25–81)
Gender	Male	23 (48)
	Female	25 (52)
Body mass index	<25	8 (16)
	25–30	10 (21)
	>30	30 (63)
Weight loss	Yes	40 (83)
	No	8 (17)
Smoke	Yes	18 (38)
	No	30 (62)

(95–105%, $R^2 > 0.99$) were validated via melting curve analysis and standard curves, respectively. RNU6 served as the stable internal control.²⁵ Cycle threshold (Ct) values were averaged across technical triplicates for each sample ($n = 48$); outliers were excluded (standard deviation [SD] > 0.5).

2.5. Statistical analysis

The data distribution was assessed using the Shapiro–Wilk test. For differential expression analysis between tumor and paired normal tissues, differences were evaluated using the paired Student's *t*-test (for normally distributed data) or the Wilcoxon matched-pairs signed-rank test (for non-normally distributed data). The relative expression levels were calculated using the comparative Ct method with the following formula: $FC = 2^{-\Delta\Delta Ct}$, where $\Delta\Delta Ct = (Ct_{\text{target}} - Ct_{\text{reference}})_{\text{tumor}} - (Ct_{\text{target}} - Ct_{\text{reference}})_{\text{normal}}$. Values > 1 indicated upregulation, whereas values < 1 indicated downregulation. To account for multiple comparisons across the four miRNA arms, the FDR was controlled using the Benjamini–Hochberg procedure. This correction was applied separately for the differential expression analysis (tissue comparisons) and the prognostic analysis (Cox models), with an FDR threshold of <0.05 considered statistically significant.

To assess the prognostic value of the mature arms of miR-182 and miR-490, 5-year OS was analyzed. This was performed in two approaches to ensure robustness: (i)

Table 2. The primer sequences used in this study

Target	Primer sequence 5'– 3'	Product length (bp)	Annealing temperature (°C)
RNU6	F: 5'-CGCTTCGGCAGCACATATACT-3' R: 5'-CGCTTCACGAATTGCGTGTG-3' SLP U6: 5'-GTCGTATCCAGTGCAGGGTCCGAGGTATTTCGCACTGGATACGACAAAAATAT-3'	90	62
mir-182-3p	F: 5'-GTGCAGGGTCCGAGGT-3' R: 5'-GATTTGGCAATGGTAGAACTCAC-3' SLP: 5'-GTCGTATCCAGTGCAGGGTCCGAGGTATTTCGCACTGGATACGAC TAGTTGGC-3'	90	58.6
mir-182-5p	F: 5'-GTGCAGGGTCCGAGGT-3' R: 5'-GATTTGGCAATGGTAGAACTCAC-3' SLP: 5'-GTCGTATCCAGTGCAGGGTCCGAGGTATTTCGCACTGGATACGAC AGTGTGAG-3'	90	58.5
mir-490-3p	F: 5'-TGTGCGTGGAAAGCGTAGCCG-3' R: 5'-AGCACATCCTGAAGACTGACT-3' SLP: 5'-GTCGTATCCAGTGCAGGGTCCGAGGTATTTCGCACTGGATACGAC CCAGCATGG-3'	70	60
mir-490-5p	F: 5'-CAGGTCAAGTGGTAGCCATGA-3' R: 5'-CACCTGGAGAGGAGGGACTGT-3' SLP: 5'-GTCGTATCCAGTGCAGGGTCCGAGGTATTTCGCACTGGATACGAC ACCACCT-3'	65	61.5

Abbreviations: F: Forward primers; R: Reverse primers; SLP: Stem-loop primer.

treating expression as a continuous variable (reporting hazard ratios [HRs] per 1-unit increase in ΔCt) to maximize information retention and assess linear trends, and (ii) dichotomizing expression into “high” and “low” groups based on the median value for Kaplan–Meier visualization. We opted against further stratification (for instance, tertiles or quartiles) given the limited sample size ($n = 48$), as this would reduce subgroup counts to levels inadequate for reliable statistical inference. The hazard function $h(t|X)$ was defined in Equation (1):

$$h(t|X) = h_0(t) \exp(\beta_1 X_1 + \dots + \beta_4 X_4) \quad (1)$$

Where $h_0(t)$ represents the baseline hazard at time t , and β denotes the regression coefficients for the covariates X (miRNA expression levels). HR and 95% confidence intervals (CI) were calculated from the model. Statistical analyses were conducted using GraphPad Prism (Version 9.0, Dotmatics, United Kingdom) (for visualization) and Python software (Version 3.10, Python Software Foundation, Netherlands) utilizing the lifelines package²⁶ for Cox modeling. Model assumptions were rigorously checked; specifically, the proportional hazards assumption was tested using Schoenfeld residuals, with no significant violations observed ($p > 0.05$).

3. Results

3.1. Gene ontology enrichment analysis

The gene ontology enrichment analysis—performed using a hypergeometric test against a background of all protein-coding genes—revealed distinct biological roles for the identified targets. For the upregulated miR-182, the intersected downregulated targets were significantly enriched in processes governing cellular motility and structural organization. Specifically, significant enrichment was observed in “movement of cell or subcellular component” ($FDR = 1.34 \times 10^{-19}$; $n = 124$ genes), “cell development” ($FDR = 4.21 \times 10^{-18}$; $n = 153$ genes), and “cell projection organization” ($FDR = 1.12 \times 10^{-17}$; $n = 98$ genes) (Figure S1-A and Table S1).

In contrast, for the tumor-suppressive miR-490, the analysis of upregulated target genes highlighted strong enrichment in cell-cycle-related processes. The results demonstrate that these targets have significant participation in the “mitotic cell cycle” ($FDR = 8.76 \times 10^{-19}$; $n = 186$ genes) and “mitotic cell cycle process” ($FDR = 2.15 \times 10^{-18}$; $n = 164$ genes) (Figure S1-B and Table S2).

3.2. Experimental study

3.2.1. Patient demographic and pathological information

Patient demographics (Table 1) indicate that most patients affected by CRC were older than 50 years (the age range of participants was 25–81, with a mean age of 52). The clinicopathological information of CRC patients, including disease symptoms and tumor, node, metastasis (TNM) staging, was collected (Table 3).

3.2.2. Mature arms of miR-182 and miR-490 expression pattern

Table 3. The clinicopathological information of colorectal cancer patients

Clinicopathological information	Category	Count (n=48)	Percentage
CEA (μg/L)	Above 3	42	87.50
	Below 3	6	12.50
Hb (g/dL)	Below 12	34	70.80
	Above 12	14	29.20
Metastasis (M)	M0 (no distant metastasis)	43	89.60
	M1 (distant metastasis)	5	10.40
Stage (TNM)	Stage I	10	20.80
	Stage II	19	39.60
	Stage III	14	29.20%
	Stage IV	5	10.40
Grade of differentiation	Well	14	29.20
	Moderate	20	41.70
	Poor	14	29.20
Depth of invasion (T)	T1	14	29.20
	T2	4	8.30
	T3	20	41.70
	T4	10	20.80
LN invasion (N)	N0 (no regional lymph node metastasis)	34	70.80
	N1 (metastasis in 1–3 regional lymph nodes)	10	20.80
	N2 (metastasis in ≥4 regional lymph nodes)	4	8.30
Tumor size (cm)	Above 4.5	18	37.50
	Below 4.5	30	62.50
LN resected	0–7	20	41.70
	8–12	16	33.30
	Above 12	12	25.00
Vascular invasion	No	34	70.80
	Yes	14	29.20
Perineural invasion	No	38	79.20
	Yes	10	20.80

Abbreviations: CEA: Carcinoembryonic antigen; Hb: Hemoglobin; LN: Lymph node; TNM: Tumor-node-metastasis classification.

Quantitative RT-PCR was used to assess the expression levels of miR-182 and miR-490, along with their respective mature 3p and 5p arms that showed differential expression in CRC tissues compared to paired NATs.

The expression of miR-182 arms was significantly elevated in CRC tissues compared to NATs (Figure 2A). Notably, miR-182-5p exhibited a mean FC of 16.19 ± 1.39 ($p < 0.001$), whereas miR-182-3p showed a mean FC of 3.38 ± 0.49 ($p = 0.032$, following FDR correction). To validate these findings, miR-182 expression was further evaluated in CRC-derived cell lines, including Caco-2 and SW480. Results indicated significant upregulation of miR-182-3p in Caco-2 cells (4.58-fold, $p < 0.001$) and SW480 cells (3.85-fold, $p < 0.001$), as well as miR-182-5p in Caco-2 cells (19.27-fold, $p < 0.001$) and SW480 cells (17.20-fold, $p < 0.001$). Overall, miR-182-5p expression was observed to be approximately 4 times greater than that of miR-182-3p across these contexts.

In contrast, miR-490 expression was significantly reduced in both CRC tissues and cell lines compared with NATs (Figure 2B). Specifically, miR-490-3p displayed a mean FC of 0.76 (downregulated 1.31-fold) ($p = 0.032$, following FDR correction), and miR-490-5p showed a mean FC of 0.26 (downregulated 3.86-fold) ($p < 0.001$) in CRC tissues compared to NATs. Consistent with tissue observations, miR-490-3p was downregulated in Caco-2 cells (0.62-fold, $p = 0.177$) and SW480 cells (0.71-fold, $p = 0.377$), though these changes did not achieve statistical significance. Conversely, miR-490-5p was markedly downregulated in Caco-2 cells (0.024-fold, $p < 0.001$) and SW480 cells (0.05-fold, $p < 0.001$).

3.2.3. Association of mature arm expression with 5-year overall survival

To evaluate the prognostic implications of miR-182 and miR-490 mature products, we conducted a survival analysis on the cohort of 48 CRC patients, using tissue expression levels quantified by quantitative RT-PCR (ΔC_t values) alongside recorded 5-year survival data. Survival times were capped at 5 years, with events defined as death ($n = 18$) and censoring at 5 years for survivors ($n = 30$). The Kaplan–Meier estimator was used to estimate overall 5-year OS, and Cox proportional hazards models assessed associations with miRNA expression, both as continuous and dichotomized at the median. The overall 5-year OS rate was 62.5% (30/48 patients censored at 5 years), consistent with rates in intermediate-stage CRC cohorts. The median follow-up time was 60 months (interquartile range: 18–60 months). Event times occurred at 1 year (4 events), 2 years (8 events), 3 years (3 events), and 4 years (3 events), with no events recorded at the 5-year mark (Figure 3).

Univariate Cox models revealed no significant linear associations between miR-182 arm expressions and survival hazard (Table 4). For miR-182-3p, the HR was 0.741 (95% CI: 0.279–1.972, $p = 0.549$ after FDR correction). For miR-182-5p, HR = 0.858 (95% CI: 0.610–1.205, $p = 0.377$ after FDR correction). In a multivariate Cox model including both arms, neither was significant ($p > 0.05$). Stratification by median expression (miR-182-3p median = 12.1967; miR-182-5p median = 8.0000) also showed no significant differences between high ($>$ median) and low (\leq median) groups via log-rank test equivalents in Cox regression.

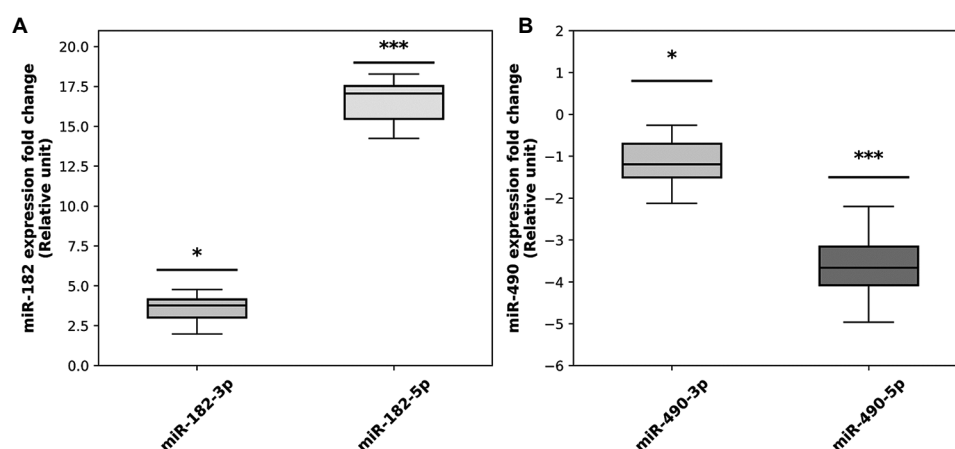


Figure 2. Expression levels of cancer-associated miRNAs in colorectal cancer (CRC) tissues. Data are presented as mean \pm standard deviation. (A) Relative expression of miR-182 in CRC tissues compared to paired normal adjacent tissues (NATs). Significant upregulation was observed for miR-182-5p ($p < 0.001$) and miR-182-3p ($p = 0.032$). (B) Relative expression of miR-490 in CRC tissues compared to NATs. Significant downregulation was noted for miR-490-3p ($p = 0.032$) and miR-490-5p ($p < 0.001$). Statistical significance was determined using the paired Student's *t*-test ($n = 48$ biological replicates per group). Notes: * $p < 0.05$; *** $p < 0.001$.

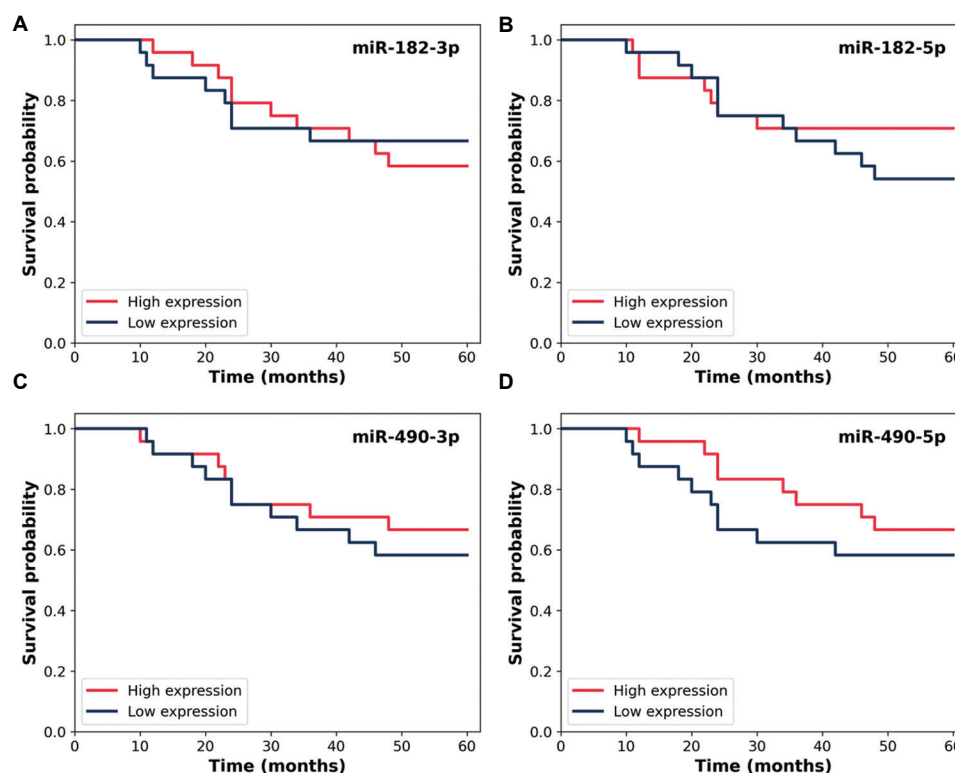


Figure 3. Kaplan–Meier survival estimates for miR-182 and miR-490 mature arms in colorectal cancer patients ($n = 48$). Patients were stratified into high (red line) and low (blue line) expression groups based on the median delta cycle threshold (ΔCT) value. The panels display overall survival probability over 60 months for (A) miR-182-3p, (B) miR-182-5p, (C) miR-490-3p, and (D) miR-490-5p. Vertical tick marks on the curves represent censored subjects (alive at last follow-up). The tables aligned below the X-axis indicate the number of patients at risk at each 12-month interval. Assessment via the log-rank test revealed no statistically significant difference in 5-year overall survival between high and low expression groups for any of the four miRNA arms ($p > 0.05$).

Table 4. Univariate Cox proportional hazards analysis for 5-year overall survival by mature arm expression

Mature miRNA	Log (HR)	HR	SE	p -value (FDR-corrected)	95% CI for HR
miR-182-3p	−0.2991	0.741	0.499	0.549	[0.279, 1.972]
miR-182-5p	−0.1534	0.858	0.174	0.377	[0.610, 1.205]
miR-490-3p	−0.4083	0.665	0.317	0.198	[0.357, 1.239]
miR-490-5p	−0.0781	0.925	0.283	0.782	[0.532, 1.610]

Abbreviations: CI: Confidence interval; FDR: False discovery rate; HR: Hazard ratio; SE: Standard error.

For high miR-182-3p, HR = 0.898 (95% CI: 0.35682–3p, i $p=0.819$). For high miR-182-5p, HR = 0.651 (95% CI: 0.257–1.650, $p=0.365$). These findings suggest miR-182 mature arms, despite their oncogenic roles in tissue dysregulation, do not strongly predict 5-year OS in this cohort.

Similarly, univariate Cox models for miR-490 arms showed no significant associations. For miR-490-3p, HR = 0.665 (95% CI: 0.357–1.239, $p=0.198$ after FDR correction). For miR-490-5p, HR = 0.925 (95% CI: 0.532–1.610, $p=0.782$ after FDR correction). Multivariate inclusion of both arms yielded non-significant results ($p > 0.05$). Median stratification (miR-490-3p median = 10.2573; miR-490-5p median = 8.9621) confirmed no differences. For high

miR-490-3p, HR = 0.814 (95% CI: 0.323–2.055, $p=0.664$). For high miR-490-5p, HR = 1.330 (95% CI: 0.516–3.430, $p=0.556$). This aligns with miR-490's tumor-suppressive function, which may not directly translate to survival impacts detectable in this sample size (Tables 4 and 5). A combined multivariate Cox model with all four mature miRNAs confirmed no significant predictors ($p > 0.05$ for all), indicating limited prognostic value in this analysis.

4. Discussion

The significant upregulation of miR-182 mature arms observed in our cohort is consistent with extensive literature firmly establishing miR-182 as a canonical

Table 5. Stratified Cox analysis (high vs. low expression at median)

Mature miRNA	Median value	Log (HR) for high	HR for high	SE	p-value (log-rank equivalent)	95% CI for HR
miR-182-3p	12.1967	-0.1080	0.898	0.472	0.819	[0.356, 2.262]
miR-182-5p	8.0000	-0.4295	0.651	0.475	0.365	[0.257, 1.650]
miR-490-3p	10.2573	-0.2053	0.814	0.472	0.664	[0.323, 2.055]
miR-490-5p	8.9621	0.2850	1.330	0.484	0.556	[0.516, 3.430]

Abbreviations: CI: Confidence interval; HR: Hazard ratio; SE: Standard error.

oncomiR in CRC and numerous other malignancies.²⁷ Previous investigations, using diverse methodologies, such as quantitative RT-PCR and *in situ* hybridization across large patient cohorts, have repeatedly documented that miR-182 expression is markedly elevated in CRC tissues compared with non-neoplastic normal mucosa.²⁸ This consistent finding across diverse study populations and analytical platforms solidifies miR-182's role as a key player in the molecular landscape of colorectal carcinogenesis. One study involving 48 cases of CRC reported that 57.25% of tumors exhibited high miR-182 expression, compared to only 25.37% in normal tissues, a highly significant difference ($p < 0.001$). Functionally, the bioinformatic prediction from the current study linking miR-182 to "movement of cell" aligns with mechanistic evidence from cancer models. Research in breast cancer has demonstrated that miR-182 directly influences cell motility by regulating actin distribution and promoting the formation of filopodia, cellular protrusions essential for invasion.²⁹ This pro-invasive function is a recurring theme, with studies showing that miR-182 upregulation contributes to enhanced tumor cell survival and metastatic behaviors in a wide array of cancers, including melanoma, glioma, and ovarian cancer.³⁰ The oncogenic activity of miR-182 is not limited to metastasis; it is a pleiotropic regulator involved in multiple hallmarks of cancer. It promotes proliferation and inhibits apoptosis, thereby contributing directly to tumor growth and survival. Furthermore, it has been implicated in angiogenesis by regulating the hypoxia-inducible factor 1 α -vascular endothelial growth factor A axis, a critical pathway for the formation of new blood vessels.³¹ This multifaceted role suggests that miR-182 functions not as a peripheral actor but as a central regulatory hub in oncogenesis, orchestrating a suite of pro-tumorigenic programs. The molecular mechanisms underlying these functions are rooted in miR-182's ability to directly target and repress multiple tumor suppressor genes. In CRC, experimental silencing of miR-182 has been shown to inhibit tumor development by inducing apoptosis, indicating that its endogenous upregulation provides a survival advantage to cancer cells. This is consistent with its well-documented role in repressing key tumor suppressors, such as forkhead box (FOX) O1

and FOXO3a, metastasis suppressor 1, and breast cancer 1 in various cancer contexts.³² Through suppressing these critical negative regulators of cell growth and survival, miR-182 effectively alleviates inhibitory control over tumorigenesis, providing a clear molecular basis for its potent oncogenic effects.

In direct opposition to the oncogenic role of miR-182, the findings of this study on miR-490 align with a growing body of evidence that characterizes it as a potent tumor suppressor in CRC.³³ The significant downregulation of both miR-490-3p and miR-490-5p in CRC tissues relative to NATs corroborates previous reports documenting their repression in CRC tissues, cell lines, and even in the plasma of CRC patients, suggesting their potential as non-invasive biomarkers.³⁴ This consistent loss of expression suggests a critical role in maintaining normal colonic epithelial homeostasis, a function disrupted during carcinogenesis.

The bioinformatic analysis in the current study, which linked miR-490 targets to the cell cycle with high statistical confidence ($\text{FDR} = 8.76 \times 10^{-19}$), is substantiated by functional experiments in the literature. Overexpression of miR-490-3p in CRC cell lines has been shown to markedly inhibit proliferation by inducing G2/M cell cycle arrest and to significantly enhance apoptosis. These findings provide a clear context for our bioinformatic results, suggesting that the loss of miR-490 expression removes a critical suppressor of the cell division machinery.

The tumor-suppressive actions of miR-490 are mediated through its direct interaction with and subsequent repression of key oncogenic target genes. One well-validated target in CRC is Voltage Dependent Anion Channel 1 (VDAC1). MiR-490-3p directly binds to the 3'-untranslated region of VDAC1, leading to a reduction in its mRNA and protein levels and subsequent inhibition of the pro-survival VDAC1/adenosine monophosphate-activated protein kinase/mechanistic target of rapamycin signaling pathway.³⁴ Another confirmed target is RAB14, a protein involved in intracellular trafficking that is overexpressed in multiple human malignancies and contributes to CRC progression. The inverse correlation observed between miR-490-3p and its oncogenic targets, such as VDAC1 and RAB14, in CRC tissues further

solidifies this regulatory axis.³⁵ An interesting aspect highlighted by both the current study and the broader literature is the coordinated tumor-suppressive action of both strands derived from the pre-miR-490 hairpin. The observation that both miR-490-3p and miR-490-5p are significantly downregulated suggests a powerful, dual-pronged mechanism of tumor suppression originating from a single genomic locus. While they possess distinct, non-overlapping sets of target genes, both contribute to an overall anti-tumorigenic effect.¹¹ This implies that any genetic or epigenetic event that silences the miR-490 locus would have a compounded deleterious effect, simultaneously removing two distinct tumor-suppressive activities. This dual-strand functionality amplifies the biological significance of its downregulation in CRC, underscoring its importance as a guardian of cellular homeostasis.

A central finding of the present study is the lack of a statistically significant association between the expression levels of any of the four measured mature miRNAs, miR-182-3p, miR-182-5p, miR-490-3p, and miR-490-5p, and 5-year OS in the cohort of 48 CRC patients. Despite their significant dysregulation in tumor tissues and their clear links to fundamental cancer pathways, neither univariate nor multivariate Cox proportional hazards models could establish these miRNAs as prognostic indicators. For instance, the HR for miR-182-5p was 0.858 (95% CI: 0.610–1.205; $p = 0.377$), and for miR-490-3p, it was 0.665 (95% CI: 0.357–1.239; $p = 0.198$), with both CIs crossing 1.0, indicating no significant effect on survival hazard. This diverges from a substantial body of published research linking the expression of these miRNAs to patient outcomes in CRC.

The disconnection between the current study's results and the existing literature is particularly evident for miR-182. Multiple independent studies have reported that its overexpression is not only a feature of CRC but is also strongly correlated with aggressive clinicopathological characteristics, including advanced T-stage, lymph node metastasis (N-stage), and distant metastasis (M-stage).³⁶ These features are powerful predictors of poor outcomes. Consequently, these studies found that high miR-182 expression was significantly associated with shorter OS. This finding has been corroborated at the meta-analytic level; a comprehensive meta-analysis that pooled data from three CRC studies calculated a combined HR of 1.99 (95% CI: 1.34–2.96), indicating that patients with high miR-182 expression have nearly double the risk of death compared to those with low expression.³⁷

A similar contradiction exists for miR-490. While the current study reported no association with OS, previous

work has consistently identified low miR-490-3p expression as a marker of poor prognosis in CRC. For example, one study reported that patients with low miR-490-3p levels had a significantly shorter OS, with a univariate HR of 2.248 (95% CI: 1.291–3.914; $p = 0.007$).³⁴ Another study involving 50 CRC cases confirmed this trend, showing that patients with elevated miR-490-3p expression had a significantly prolonged OS in Kaplan–Meier analysis.³⁵ The divergence between our findings and the established literature is likely attributable to multiple methodological limitations and complex biological factors known to influence biomarker studies.³⁸

The primary limitation is the small cohort size ($n = 48$), with only 18 recorded deaths, leaving the survival analysis underpowered to detect modest effects. This statistical uncertainty is reflected in the wide CIs reported in our Cox analysis (e.g., crossing 1.0), indicating that the available data cannot definitively resolve the actual effect size. Second, the molecular and clinical heterogeneity of the patient sample is a major confounding factor. The study cohort included patients with various tumor stages and grades. However, it was not stratified by crucial molecular classifiers, such as CMS, microsatellite instability status, or primary tumor location. A genuine prognostic effect within a specific subgroup could therefore be masked or diluted when analyzed across this heterogeneous population. Finally, the analysis is confounded by unrecorded biological and clinical variables. The biological impact of a miRNA is contingent on the broader cellular and molecular context, including the tumor's specific mutational landscape and the balance of competing endogenous RNA networks, which have not been assessed. Notably, the lack of data on patient treatment protocols is a significant oversight. Without the ability to adjust for therapeutic interventions, it is impossible to disentangle the intrinsic prognostic value of the miRNAs from the powerful influence of treatment on OS.

In addition, technical differences in miRNA quantification may contribute to the discrepancy. We utilized stem-loop quantitative RT-PCR, which detects the dominant mature sequence but may not distinguish between length-variant mature arms that differ by 1–2 nucleotides at the ends. Since specific mature arms variants can have distinct half-lives and target specificities, future research utilizing small RNA sequencing is necessary to capture the full complexity of the mature arms landscape.

These limitations dictate clear directions for future research. To definitively assess the prognostic value of these molecules, future studies should utilize small RNA sequencing rather than quantitative RT-PCR to capture the full complexity of the mature miRNA landscape. Furthermore, validation should be conducted in larger,

multi-centered cohorts with comprehensive clinical annotation to allow for multivariate adjustment for treatment effects and molecular subtypes.

5. Conclusion

In conclusion, this study validated the opposing dysregulation of mature miR-182 and miR-490 arms in CRC, reinforcing their roles as putative oncomiRs and tumor suppressors, respectively. While bioinformatics analyses linked these changes to cell motility and mitotic cell cycle pathways, this dysregulation did not translate into a statistically significant association with 5-year OS in our cohort. This discrepancy highlights the limitations of standard stem-loop quantitative RT-PCR, which targets the dominant mature sequence rather than specific isomiR variants, as well as the constraints of a limited sample size. Consequently, we recommend that future research utilize small RNA sequencing to capture the full complexity of the mature arms landscape and validate these findings in larger, multi-centered cohorts to definitively detect modest prognostic effects.

Acknowledgments

The Center for International Scientific Studies & Collaboration (CISSC), the Ministry of Science, Research, and Technology, and the NIGEB have provided the equipment for this work. The authors thank the Imam Khomeini Hospital Complex for providing patient samples.

Funding

This project is financially supported by the Center for International Scientific Studies and Collaboration (CISSC) with approval number 737.

Conflict of interest

The authors declare they have no competing interests.

Author contributions

Conceptualization: Shahla Mohammad Ganji, Majid Pornour

Formal analysis: Shahla Mohammad Ganji, Arash Moradi

Investigation: Arash Moradi, Seyedeh Hanieh Safavi Komamardakhi, Ramtin Mohammadi, Azar Heidarizadi, Mahmoud Hatami

Methodology: Shahla Mohammad Ganji, Mariasanta Napolitano, Arash Moradi

Writing–original draft: Arash Moradi, Ramtin Mohammadi

Writing–review & editing: Shahla Mohammad Ganji, Arash Moradi

Ethics approval and consent to participate

This study was approved by the National Institute of

Genetic Engineering and Biotechnology (NIGEB) Ethics Committee (approval number IR.NIGEB.EC.1397.8.1.G). All patients provided written informed consent before participation.

Consent for publication

Not applicable.

Availability of data

All data were obtained from <https://www.mirnet.ca/andhttp://gepia2.cancer-pku.cn>.

References

1. Bray F, Laversanne M, Sung H, *et al*. Global cancer statistics 2022: GLOBOCAN estimates of incidence and mortality worldwide for 36 cancers in 185 countries. *CA Cancer J Clin*. 2024;74(3):229-263.
doi: 10.3322/caac.21834
2. Anyane-Yeboah A, Bermudez H, Fredericks M, *et al*. The revised colorectal cancer screening guideline and screening burden at community health centers. *Sci Rep*. 2025;15(1):336.
doi: 10.1038/s41598-024-83343-1
3. Lhewa DY, Strate LL. Pros and cons of colonoscopy in management of acute lower gastrointestinal bleeding. *World J Gastroenterol*. 2012;18(11):1185-1190.
doi: 10.3748/wjg.v18.i11.1185
4. Chen B, Xia Z, Deng YN, *et al*. Emerging microRNA biomarkers for colorectal cancer diagnosis and prognosis. *Open Biol*. 2019;9(1):180212.
doi: 10.1098/rsob.180212
5. Keum N, Giovannucci E. Global burden of colorectal cancer: Emerging trends, risk factors and prevention strategies. *Nat Rev Gastroenterol Hepatol*. 2019;16(12):713-732.
doi: 10.1038/s41575-019-0189-8
6. Guinney J, Dienstmann R, Wang X, *et al*. The consensus molecular subtypes of colorectal cancer. *Nat Med*. 2015;21(11):1350-1356.
doi: 10.1038/nm.3967
7. Esteller M. Non-coding RNAs in human disease. *Nat Rev Genet*. 2011;12(12):861-874.
doi: 10.1038/nrg3074
8. Ambros V. microRNAs: Tiny regulators with great potential. *Cell*. 2001;107(7):823-826.
doi: 10.1016/s0092-8674(01)00616-x
9. Shivdasani RA. MicroRNAs: Regulators of gene expression and cell differentiation. *Blood*. 2006;108(12):3646-3653.
doi: 10.1182/blood-2006-01-030015

10. Shi W, Wartmann T, Accuffi S, *et al.* Integrating a microRNA signature as a liquid biopsy-based tool for the early diagnosis and prediction of potential therapeutic targets in pancreatic cancer. *Br J Cancer*. 2024;130(1):125-134.
doi: 10.1038/s41416-023-02488-4
11. Gahlawat AW, Witte T, Sinn P, Schott S. Circulating cf-miRNA as a more appropriate surrogate liquid biopsy marker than cfDNA for ovarian cancer. *Sci Rep*. 2023;13(1):5503.
doi: 10.1038/s41598-023-32243-x
12. Rao BH, Bouskova V, Heczko L, *et al.* Comprehensive transcriptome and miRNome profiling in metachronous colorectal liver metastasis: Insight into the prognostic and molecular subtypes. *Lab Invest*. 2025;106:104274.
doi: 10.1016/j.labinv.2025.104274
13. Guo L, Yu J, Yu H, *et al.* Evolutionary and expression analysis of miR-#-5p and miR-#-3p at the miRNAs/isomiRs levels. *Biomed Res Int*. 2015;2015:168358.
doi: 10.1155/2015/168358
14. Peng Y, Croce CM. The role of MicroRNAs in human cancer. *Signal Transduct Target Ther*. 2016;1(1):15004.
doi: 10.1038/sigtrans.2015.4
15. Hanahan D, Weinberg RA. Hallmarks of cancer: The next generation. *Cell*. 2011;144(5):646-674.
doi: 10.1016/j.cell.2011.02.013
16. Hwang HW, Mendell JT. MicroRNAs in cell proliferation, cell death, and tumorigenesis. *Br J Cancer*. 2006;94(6):776-780.
doi: 10.1038/sj.bjc.6603023
17. He X, Dong Y, Wu CW, *et al.* MicroRNA-218 inhibits cell cycle progression and promotes apoptosis in colon cancer by downregulating BMI1 polycomb ring finger oncogene. *Mol Med*. 2013;18(1):1491-1498.
doi: 10.2119/molmed.2012.00304
18. Wu CW, Evans JM, Huang S, *et al.* A comprehensive approach to sequence-oriented IsomiR annotation (CASMIR): Demonstration with IsomiR profiling in colorectal neoplasia. *BMC Genomics*. 2018;19(1):401.
doi: 10.1186/s12864-018-4794-7
19. Franco S, Pluvinet R, Sanchez-Herrero JF, Sumoy L, Martinez MA. Rapid and accurate quantification of isomiRs by RT-qPCR. *Sci Rep*. 2022;12(1):17220.
doi: 10.1038/s41598-022-22298-7
20. Kramer MF. Stem-loop RT-qPCR for miRNAs. *Curr Protoc Mol Biol*. 2011;Chapter 15:Unit 15 10.
doi: 10.1002/0471142727.mb1510s95
21. Chang L, Zhou G, Soufan O, Xia J. miRNet 2.0: Network-based visual analytics for miRNA functional analysis and systems biology. *Nucleic Acids Res*. 2020;48(W1):W244-W251.
doi: 10.1093/nar/gkaa467
22. Tang Z, Kang B, Li C, Chen T, Zhang Z. GEPIA2: An enhanced web server for large-scale expression profiling and interactive analysis. *Nucleic Acids Res*. 2019;47(W1):W556-W560.
doi: 10.1093/nar/gkz430
23. Ge SX, Jung D, Yao R. ShinyGO: A graphical gene-set enrichment tool for animals and plants. *Bioinformatics*. 2020;36(8):2628-2629.
doi: 10.1093/bioinformatics/btz931
24. Nagtegaal ID, Odze RD, Klimstra D, *et al.* The 2019 WHO classification of tumours of the digestive system. *Histopathology*. 2020;76(2):182-188.
doi: 10.1111/his.13975
25. Soheilifar MH, Vaseghi H, Seif F, *et al.* Concomitant overexpression of mir-182-5p and mir-182-3p raises the possibility of IL-17-producing Treg formation in breast cancer by targeting CD3d, ITK, FOXO1, and NFATs: A meta-analysis and experimental study. *Cancer Sci*. 2021;112(2):589-603.
doi: 10.1111/cas.14764
26. Davidson-Pilon C. Lifelines: Survival analysis in Python. *J Open Source Softw*. 2019;4(40):1317.
doi: 10.21105/joss.01317
27. Sameti P, Tohidast M, Amini M, Bahojb Mahdavi SZ, Najafi S, Mokhtarzadeh A. The emerging role of MicroRNA-182 in tumorigenesis; a promising therapeutic target. *Cancer Cell Int*. 2023;23(1):134.
doi: 10.1186/s12935-023-02972-0
28. Popa ML, Ichim C, Anderco P, Todor SB, Pop-Lodromanean D. MicroRNAs in the diagnosis of digestive diseases: A comprehensive review. *J Clin Med*. 2025;14(6):2054.
doi: 10.3390/jcm14062054
29. Li X, Zhang X, Zhang Q, Lin R. miR-182 contributes to cell proliferation, invasion and tumor growth in colorectal cancer by targeting DAB2IP. *Int J Biochem Cell Biol*. 2019;111:27-36.
doi: 10.1016/j.biocel.2019.04.002
30. Zehtabi M, Ghaedrahmati F, Dari MAG, *et al.* Emerging biologic and clinical implications of miR-182-5p in gynecologic cancers. *Clin Transl Oncol*. 2025;27(6):2367-2382.
doi: 10.1007/s12094-024-03822-9
31. Kokaine L, Daneberga Z, Satcs M, *et al.* The prognostic role of microRNAs 142-5p, 182-3p, and 99a-3p in locally advanced rectal cancer patients. *Anticancer Res*. 2025;45(9):3895-3912.
doi: 10.21873/anticancer.17748
32. Kandil NS, Kandil LS, Mohamed R, *et al.* The role of

- miRNA-182 and FOXO3 expression in breast cancer. *Asian Pac J Cancer Prev*. 2022;23(10):3361-3370.
doi: 10.31557/APJCP.2022.23.10.3361
33. Vinchure OS, Kulshreshtha R. miR-490: A potential biomarker and therapeutic target in cancer and other diseases. *J Cell Physiol*. 2021;236(5):3178-3193.
doi: 10.1002/jcp.30119
34. Liu X, He B, Xu T, *et al*. MiR-490-3p functions as a tumor suppressor by inhibiting oncogene VDACL1 expression in colorectal cancer. *J Cancer*. 2018;9(7):1218-1230.
doi: 10.7150/jca.23662
35. Wang B, Yin M, Cheng C, *et al*. Decreased expression of miR4903p in colorectal cancer predicts poor prognosis and promotes cell proliferation and invasion by targeting RAB14. *Int J Oncol*. 2018;53(3):1247-1256.
doi: 10.3892/ijo.2018.4444
36. Zhu X, Lin SQ, Xie J, *et al*. Biomarkers of lymph node metastasis in colorectal cancer: Update. *Front Oncol*. 2024;14:1409627.
doi: 10.3389/fonc.2024.1409627
37. Wang F, Zhong S, Zhang H, *et al*. Prognostic value of MicroRNA-182 in cancers: A meta-analysis. *Dis Markers*. 2015;2015:482146.
doi: 10.1155/2015/482146
38. Mayeux R. Biomarkers: Potential uses and limitations. *NeuroRx*. 2004;1(2):182-188.
doi: 10.1602/neurorx.1.2.182